ЖЭТФ, 2020, том 158, вып. 1 (7), стр. 17–23

COMPOSITE TOPOLOGICAL OBJECTS IN TOPOLOGICAL SUPERFLUIDS

G. E. Volovik*

Low Temperature Laboratory, Aalto University
FI-00076, Aalto, Finland

Landau Institute for Theoretical Physics, Russian Academy of Sciences
142432, Chernogolovka, Moscow Region, Russia

Received December 15, 2019,
revised version December 15, 2019
Accepted for publication March 3, 2020

Contribution for the JETP special issue in honor of A. S. Borovik-Pomanov's 100th anniversary

DOI: 10.31857/S0044451020070020

The spontaneous phase coherent precession of magnetization, discovered in 1984 by Borovik-Romanov, Bunkov, Dmitriev and Mukharskiy [1] in collaboration with Fomin [2] became now an important experimental tool for study complicated topological objects in superfluid ^{3}He.

Superfluid phases of ^{3}He discovered in 1972 [3] opened the new area for the application of topological methods to condensed matter systems. Due to the multi-component order parameter which characterises the broken SO(3) × SO(3) × U(1) symmetry in these phases, there are many textures and defects in the order parameter field, which are protected by topology. Among them there are quantized vortices, skyrmions and merons, solitons and vortex sheets, monopoles and boojums, Alice strings, Kibble–Lazarides–Shafi (KLS) walls terminated by Alice strings, spin vortices with soliton tails, etc [4]. Most of them have been experimentally identified and investigated using nuclear magnetic resonance (NMR) technique, and in particular the phase coherent spin precession discovered in 1984 in ^{3}He-B [1, 2, 5]. Such precessing state, which has got the name homogeneously precessing domain (HPD), is the spontaneously emerging steady state of precession, which preserves the phase coherence across the whole sample even in the absence of energy pumping and even in an inhomogeneous external magnetic field. It has all the signatures of the Bose–Einstein condensate of magnons (see review [6]).

In bulk liquid ^{3}He there are two topologically different superfluid phases, ^{3}He-A and ^{3}He-B [7]. One is the chiral superfluid ^{3}He-A with topologically protected Weyl points in the quasiparticle spectrum. In the ground state of ^{3}He-A the order parameter matrix has the form $A_{\alpha i} = \Delta_A e^{i\Phi} \hat{d}_\alpha (\hat{e}^i_1 + i\hat{e}^i_2)$, where $\hat{\mathbf{d}}$ is the unit vector of the anisotropy in the spin space due to spontaneous breaking of $SO(3)_S$ symmetry of spin rotations; $\hat{\mathbf{e}}_1$ and $\hat{\mathbf{e}}_2$ are mutually orthogonal unit vectors; and $\hat{\mathbf{l}} = \hat{\mathbf{e}}_1 \times \hat{\mathbf{e}}_2$ is the unit vector of the anisotropy in the orbital space due to spontaneous breaking of orbital rotations $SO(3)_L$ symmetry. The $\hat{\mathbf{l}}$-vector also shows the direction of the orbital angular momentum of the chiral superfluid, which emerges due to spontaneous breaking of time reversal symmetry. The chirality of ^{3}He-A has been probed in several experiments. [8–10]

Another phase is the fully gapped time reversal invariant ^{3}He-B. In the ground state of ^{3}He-B the order parameter matrix has the form $A_{\alpha i} = \Delta_B e^{i\Phi} R_{\alpha i}$, where $R_{\alpha i}$ is the real matrix of rotation, $R_{\alpha i} R_{\alpha j} = \delta_{ij}$. This phase has topologically protected gapless Majorana fermions living on the surface, see reviews [11, 12].

In ^{3}He confined in the nematically ordered aerogel (nafen), new phase becomes stable — the polar phase of ^{3}He [13, 14], whith the order parameter

$$A_{\alpha i} = \Delta_P e^{i\Phi} \hat{d}_\alpha \hat{m}_i \,. \qquad (1)$$

where orbital vector $\hat{\mathbf{m}}$ is fixed by the nafen strands. The polar phase in nafen obeys the analog of the Anderson theorem for the columnar defects (nafen strands),

* E-mail: volovik@boojum.hut.fi

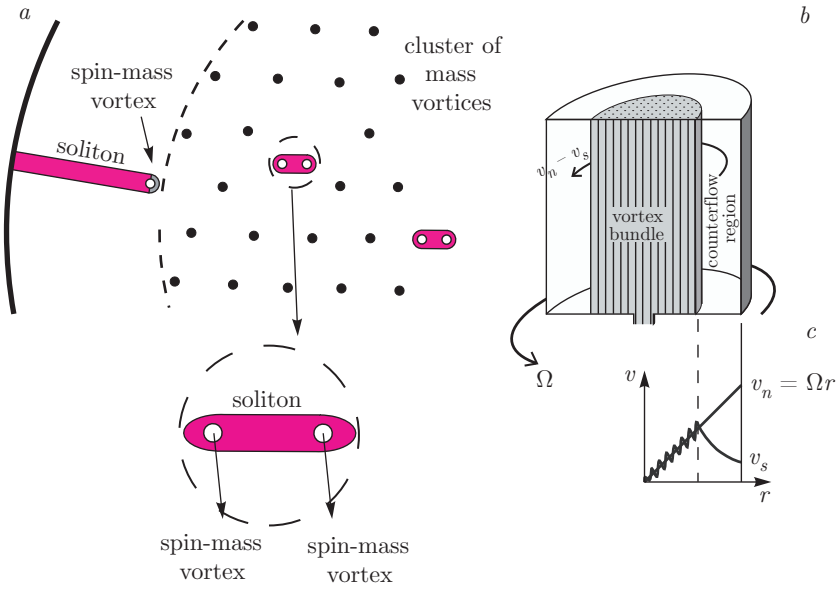

Fig. 1. *a*) Vortex cluster in rotating container with the vortex free region outside the cluster. Vortex cluster is formed when starting with the equilibrium vortex state in the rotating container the angular velocity of rotation is increased. The new vortices are not formed if the counterflow in the vortex region does not exceed the critical velocity for vortex formation. *b*) The spin-mass vortex finds its equibrium position on the periphery of the vortex cluster, where the soliton tension is compensated by the Magnus force acting on the mass vortex part of the composite object. The size of the soliton is given by Eq. (2), and this dependence on the angular velocity of rotation is confirmed by the HPD spectroscopy. *c*) The combined object with $\mathcal{N} = 2$ quanta of circulation: spin-mass vortex + soliton + spin-mass vortex

see Refs. [15, 16]. The polar phase is the time reversal invariant superfluid, which contains Dirac nodal ring in the fermionic spectrum [16, 17].

Among the topological defects in ^{3}He-B, there are the conventional mass vortices with the integer $\mathcal{N}$ winding number of the phase Φ, and the Z_2 spin vortex — the nontrivial winding of the matrix $R_{\alpha i}$. Due to spin-orbit coupling the spin vortex serves as the termination line of the topological soliton wall. Because of the soliton tension the spin vortex moves to the wall of the vessel and escapes the observation. However, the help comes from the mass vortices. The mass and spin vortices are formed by different fields. They do not interact since they "live in different worlds". The only instance, where the spin and mass vortices interact, arises when the cores of a spin and a mass vortex happen to get close to each other and it becomes energetically preferable for them to form a common core. Thus by trapping the spin vortex on a mass vortex the combined core energy is reduced and a composite object Z_2-string + soliton + mass vortex, or spin-mass vortex is formed. This object is stabilized near the edge of the vortex cluster in the rotating cryostat, see Fig. 1.

These combined objects have been observed and studied using HPD spectroscopy [18, 19]. The additional absorption observed in the HPD is proportional to the soliton area $A = lh$, where h is the height of the container, and l is the distance between the spin vortex and the wall of container, i. e. the width of the counterflow vortex-free zone. The latter is regulated by changing the angular velocity of rotation Ω at fixed number N of vortices in the cell:

$$l(\Omega) = R\left(1 - \sqrt{\frac{\Omega_V(N)}{\Omega}}\right). \qquad (2)$$

Here R is the radius of the cylindrical container, and $\Omega_V(N)$ is the angular velocity in the state in the rotating container with equilibrium number of vortices $N = 2\pi R^2\Omega_V(N)/\kappa$. The equilibtium state is obtained by cooling through T_c under rotation, and then we increase the angular velocity of rotation, $\Omega > \Omega_V(N)$. The new vortices are not created because of high energy barrier, and as a result the counterflow region appears. The dependence of the relaxation of the HPD state follows Eq. (2) [18, 19].

Among the topological defects in ^{3}He-A, is the half-quantum vortex (HQV) [20] — the condensed matter analog of the Alice string in particle physics [21].

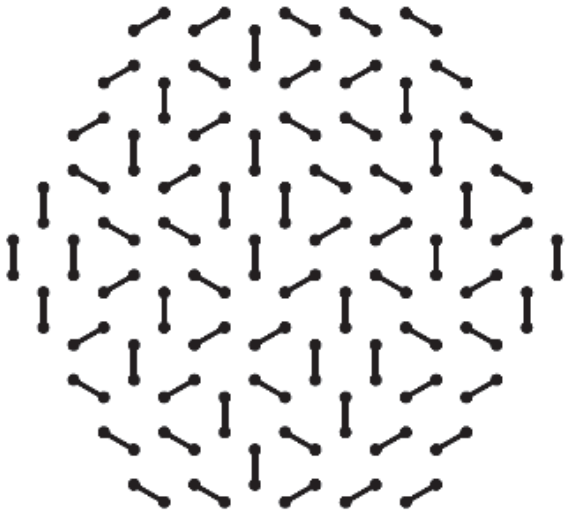

Fig. 2. Illustration of the lattice of solitons emerging between the Alice strings (HQVs) in the polar phase of ^{3}He, when the magnetic field is tilted with respect of the aerogel strands. The HQVs survive the soliton tension because they are pinned by the strands. The NMR measurements give information on the total length of the soliton and thus on the number of the Alice strings in the cell

The HQV is the vortex with fractional circulation of superfluid velocity. Its order parameter is

$$\hat{\mathbf{d}}(\hat{\mathbf{r}})e^{i\Phi(\hat{\mathbf{r}})} = \left(\hat{\mathbf{x}}\cos\frac{\phi}{2} + \hat{\mathbf{y}}\sin\frac{\phi}{2}\right)e^{i\phi}\,. \qquad (3)$$

When the azimuthal coordinate ϕ changes from 0 to 2π along the circle around this object, the vector $\hat{\mathbf{d}}(\hat{\mathbf{r}})$ changes sign and simultaneously the phase Φ changes by π, giving rise to $\mathcal{N} = 1/2$. The order parameter (3) remains continuous along the circle. While a particle that moves around an Alice string flips its charge, the quasiparticle moving around the HQV flips its spin quantum number. This gives rise to the Aharonov–Bohm effect for spin waves in NMR experiments [22].

The HQVs were first observed in the polar phase [23]. In ^{3}He-A the spin-orbit interaction leads to formation of spin soliton interpolating between two degenerate vacua with $\hat{\mathbf{d}} = \hat{\mathbf{l}}$ and $\hat{\mathbf{d}} = -\hat{\mathbf{l}}$. The energy of soliton prevents the nucleation of the Alice strings in ^{3}He-A. In contrast, in the polar phase in the absence of magnetic field, or if the field is along the nafen strands, the solitons are not formed, and HQVs are energetically most favourable vortices in rotating container. Thus they appear if the sample is cooled down from the normal state under rotation. Then, if magnetic field is tilted with respect to aerogel strands, the spin solitons are formed between the HQVs, as in A-phase. But HQVs are remained pinned by the nafen strands, see Fig. 2. The NMR absorption from excitation of spin waves localized on solitons allows to identify the HQVs and measure their density [23]. Due to the strong pinning, the Alice strings formed in the polar phase, survive after transition to the A-phase [24].

In ^{3}He-B, spin solitons give rise to doubly quantized vortices ($\mathcal{N} = 2$) — a pair of spin-mass vortices forms a molecule, where the soliton serves as chemical bond, see Fig. 1*c*. Such vortex molecules have been identified in HPD spectroscopy [18, 19].

The "conventional" $\mathcal{N} = 1$ vortex has also an unusual structure in ^{3}He-B. Already in the first experiments with rotating ^{3}He-B the first order phase transition has been observed, which has been associated with the transition inside the vortex core [25]. At the transition the vortex core becomes non-axisymmetric [26,27]. Spontaniously broken axial symmetry of the vortex was confirmed in the further HPD experiments [28]. Such vortex can be considered as two half-quantum vortices in Fig. 3 connected by the domain wall [29, 30] — the analog of the Kibble–Lazarides–Shafi wall bounded by cosmic strings [31]. The topological classification of such combined objects in terms of relative homotopy groups in the polar distorted B-phase see in Ref. [32] The phenomenon of the symmetry breaking in the core of the topological defect has been discussed for cosmic strings [33]. For the ^{3}He-B vortices, the broken SO(2) symmetry leads to the Goldstone bosons — the modes in which the axis of anisotropy $\mathbf{b}$ of the core is oscillating.

The HPD state, has been used to study the structure and twisting dynamics of this non-axisymmetric core. The coherent precession of magnetization excites the vibrational Goldstone mode via spin-orbit interaction. Moreover, due to spin-orbit interaction the precessing magnetization rotates the core around its axis with constant angular velocity. In addition, since the core was pinned on the top and the bottom of the container, it was possible even to screw the core, see Fig. 3. The twisted core corresponds to the Witten superconducting string with the electric supercurrent along the core. The rigidity of twisted core differs from that of the straight core, which is clearly seen in HPD experiments in Fig. 3. Oscillations of the vortex core under coherent spin precession lead to the observed radiation of acoustic magnon modes [34].

In the vortices with asymmetric cores the equilibrium distance between the HQVs (Alice strings) is rather small. The essentially larger KLS walls between

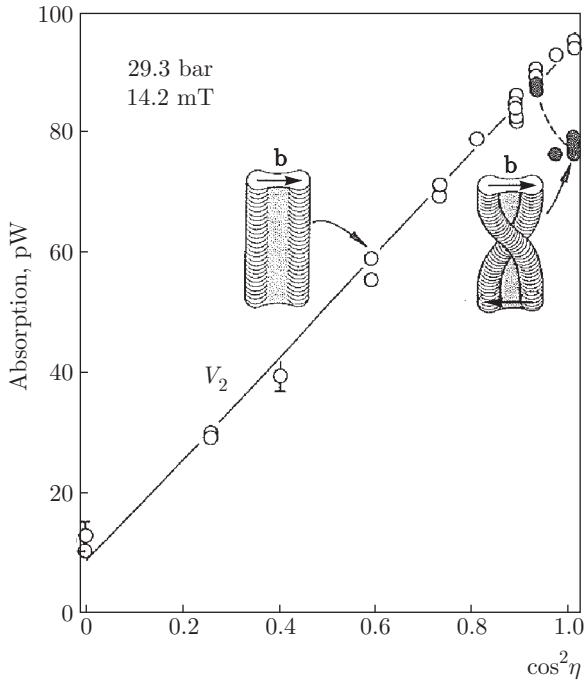

Fig. 3. The vortex in ^{3}He-B with the non-axisymmetric core represents the pair of Alice strings connected by Kibble–Lazarides–Shafi wall. The core can be twisted by applying HPD with its coherent precession of magnetization. The vortex with twisted core is analogous to Witten superconducting string with the electric current along the string core [33]. Figure shows HPD absorption as the function of the tilting angle η of magnetic field in case of the Witten strings with twisted core (filled circles) and strings with untwisted core (open circles). The estimated critical angle at which the tilted field prevents twisting by HPD is in agreement with experiment

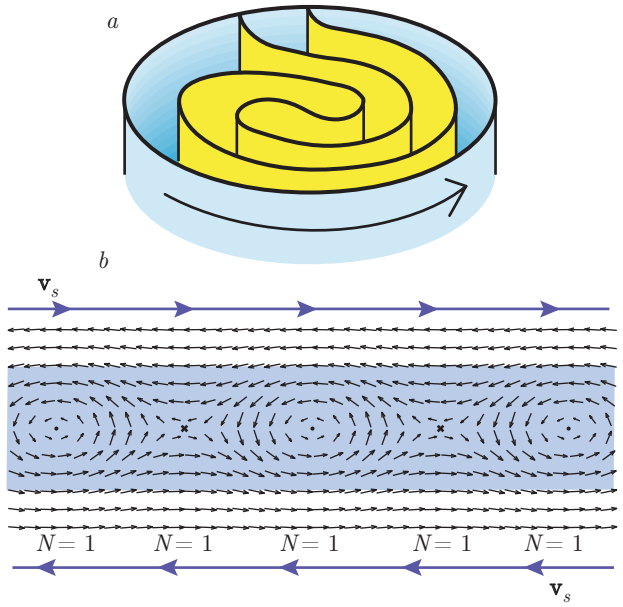

Fig. 4. *a*) Typical vortex sheet in ^{3}He-A in rotating container. It mimics the system of the equidistant cylindrical vortex sheets suggested by Landau and Lifshitz for the descrption of the rotating superfluid [44]. *b*) The element of the vortex sheet in ^{3}He-A. The vortex sheet is the soliton, which contains kinks in terms of merons. Each meron has circulation quantum $N = 1$. There are different scenarios in which vortex sheets with different geometries are prepared in the experiments [41]

the strings have been observed in the B-phase in nafen [24]. It appeared that the Alice strings formed in the polar phase survive the transition to the B-phase. They remain pinned, in spite of the formation of the KLS walls between them. This allows us to study the unique properties of the KLS wall. In particular, the KLS wall separates two degenerate vacua with different signs of the tetrad determinant, and thus between the "space-time" and "antispacetime" [35].

In the A-phase, the superfluid velocity $\mathbf{v}_s$ of the chiral condensate is determined not only by the phase Φ, but also by the orbital triad $\hat{\mathbf{e}}_1$, $\hat{\mathbf{e}}_2$ and $\hat{\mathbf{l}}$:

$$\mathbf{v}_s = \frac{\hbar}{2m}\left(\nabla\Phi + \hat{\mathbf{e}}_1^i \nabla \hat{\mathbf{e}}_2^i\right), \qquad (4)$$

where m is the mass of the ^{3}He atom. As distinct from the non-chiral superfluids, where the vorticity is presented in terms of the quantized singular vortices with the phase winding $\Delta\Phi = 2\pi\mathcal{N}$ around the vortex core, in ^{3}He-A the vorticity can be continuous. The continuous vorticity is represented by the texture of the unit vector $\hat{\mathbf{l}}$ according to the Mermi–Ho relation [36]:

$$\nabla \times \mathbf{v}_s = \frac{\hbar}{4m} e_{ijk} \hat{l}_i \nabla \hat{l}_j \times \nabla \hat{l}_k \,. \qquad (5)$$

Experimentally the continuous vorticity is typically observed in terms of skyrmions (or the Anderson–Toulouse–Chechetkin vortices [37, 38]), see the upper part of Fig. 5. Each skyrmion has $\mathcal{N} = 2$ quanta of circulation of superfluid velocity. The skyrmion can be also presented as the combination of two merons with $\mathcal{N} = 1$ each.

In 1994 a new type of continuous vorticity has been observed in ^{3}He-A — the vortex texture in the form of the vortex sheets [39–41], see Fig. 4*a* with a single vortex sheet in container. Vortex sheet is the topological soliton with kinks, each kink representing the meron — the continuous Mermin–Ho vortex with $\mathcal{N} = 1$ circulation of superfluid velocity, Fig. 4*b*. In principle, using the vortex sheet one may construct the continuous vortices with arbitrary even number $\mathcal{N} = 2k$ circulation quanta. This is the soliton in the form of

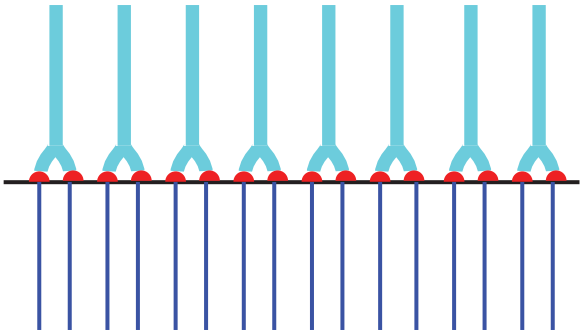

Fig. 5. Skyrmion in the A-phase splits into two merons. Each meron is terminated by boojum — the point topological objects, which lives at the interface between A-phase and B-phase. Boojum also plays the role of the Nambu monopole, which terminates the string — the $N = 1$ vortex on the B-side of the interface

closed cylindrical surface, which contains $\mathcal{N}$ "quarks" — merons [42, 43].

Another object which is waiting for its observation in ^{3}He-A is the vortex terminated by hedgehog [45,46]. This is the condensed matter analog of the electroweak magnetic monopole (Nambu monopoles [47]) or the other monopoles connected by strings [48]. The hedgehog-monopole, which terminates the vortex, exists in particular at the interface between ^{3}He-A and ^{3}He-B [49], see Fig. 5. In general, the topological defects living on the surface of the condensed matter system or at the interfaces are called boojums [50]. Boojums are classified in terms of relative homotopy groups [51]. The vortex terminated by the hedgehog-monopole was observed in cold gases [52]. The HPD state has its own topological defects [53], and among them are the spin and orbital monopoles connected by string. Several monopoles connected by strings may form the multi-monopole objects, such as necklace [54].

In ^{3}He-A the analogs of Nambu monopoles and Alice strings may form the more complex combinations. This is because the monopole serves as a source or sink of $\mathcal{N} = 2$ circulation quanta, and thus can be the termination point of 4 Alice strings with $\mathcal{N} = 1/2$ each. This in particular allows construct lattices of monopoles, in Fig. 6.

Here we considered several types of the topological confinement. The composite topological objects were experimentally observed in superfluid ^{3}He by using the unique phenomenon of HPD — the spontaneously formed coherent precession of magnetization discovered by the Borovik-Romanov group in Kapitza Institute for Physical Problems. With HPD spectroscopy, two key objects have been identified in ^{3}He-B: spin-mass

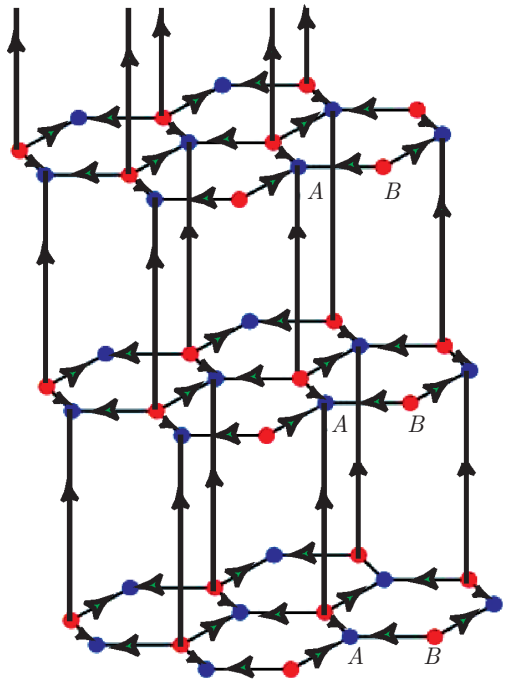

Fig. 6. (Color online) Three dimensional lattice of monopoles (on sites A) and anti-monopoles (on sites B), which are joined together by Alice strings (half-quantum vortices). Each monopole is the source or sink of 4 strings

vortex [Z_2 spin vortex + soliton+mass vortex] and non-axisymmetric vortex [Alice string + Kibble–Lazarides–Shafi wall + Alice string]. One may expect the other more complicated examples of the topological confinement of the objects of different dimensions. The complicated composite objects, such as nexus, live also in the momentum space of topological materials [55].

Funding. This work has been supported by the European Research Council (ERC) under the European Union's Horizon 2020 research and innovation programme (Grant Agreement № 694248).

Acknowledgements. I thank Q. Shafi for the discussions that ultimately led to this article.

The full text of this paper is published in the English version of JETP.

REFERENCES

1. A. S. Borovik-Romanov, Yu. M. Bunkov, V. V. Dmitriev, and Yu. M. Mukharskiy, JETP Lett. **40**, 1033, (1984).

2. I. A. Fomin, JETP Lett. **40**, 1037 (1984).

3. D. D. Osheroff, R. C. Richardson, and D. M. Lee, Phys. Rev. Lett. **28**, 885 (1972).

4. G. E. Volovik, *The Universe in a Helium Droplet*, Clarendon Press, Oxford (2003).

5. A. S. Borovik-Romanov, Yu. M. Bunkov, V. V. Dmitriev, and Yu. M. Mukharskiy, JETP **61**, 1199 (1985).

6. Yu. M. Bunkov and G. E. Volovik, in *Novel Superfluids*, ed. by K. H. Bennemann and J. B. Ketterson, Int. Ser. of Monographs on Physics **156**, Vol. 1, ch. 4, pp. 253–311 (2013).

7. D. Vollhardt and P. Wölfle, *The Superfluid Phases of Helium 3*, Dover Publ. (2013).

8. P. M. Walmsley and A. I. Golov, Phys. Rev. Lett. **109**, 215301 (2012).

9. H. Ikegami, Y. Tsutsumi, and K. Kono, Science **341**, 59 (2013).

10. H. Ikegami, Y. Tsutsumi, and K. Kono, J. Phys. Soc. Jpn. **84**, 044602 (2015).

11. T. Mizushima, Ya. Tsutsumi, M. Sato, and K. Machida, J. Phys.: Condens. Matter **27**, 113203 (2015).

12. T. Mizushima, Ya. Tsutsumi, T. Kawakami, M. Sato, M. Ichioka, and K. Machida, J. Phys. Soc. Jpn. **85**, 022001 (2016).

13. V. V. Dmitriev, A. A. Senin, A. A. Soldatov, and A. N. Yudin, Phys. Rev. Lett. **115**, 165304 (2015).

14. W. P. Halperin, J. M. Parpia, and J. A. Sauls, Phys. Today **71**, 11, 30 (2018).

15. И. А. Фомин, ЖЭТФ **154**, 1034 (2018) [I. A. Fomin, JETP **127**, 933 (2018)].

16. V. B. Eltsov, T. Kamppinen, J. Rysti, and G. E. Volovik, arXiv:1908.01645.

17. G. E. Volovik, Pis'ma v ZhETF **107**, 340 (2018) [JETP Lett. **107**, 324 (2018)].

18. Y. Kondo, J. S. Korhonen, M. Krusius, V. V. Dmitriev, E. V. Thuneberg, and G. E. Volovik, Phys. Rev. Lett. **68**, 3331 (1992).

19. J. S. Korhonen, Y. Kondo, M. Krusius, E. V. Thuneberg, and G. E. Volovik, Phys. Rev. B **47**, 8868 (1993).

20. G. E. Volovik and V. P. Mineev, JETP Lett. **24**, 561 (1976).

21. A. S. Schwarz, Nucl. Phys. B **208**, 141 (1982).

22. M. M. Salomaa and G. E. Volovik, Rev. Mod. Phys. **59**, 533 (1987).

23. S. Autti, V. V. Dmitriev, V. B. Eltsov, J. Mäkinen, G. E. Volovik, A. N. Yudin, and V.V. Zavjalov, Phys. Rev. Lett. **117**, 255301 (2016).

24. J. T. Mäkinen, V. V. Dmitriev, J. Nissinen, J. Rysti, G. E. Volovik, A. N. Yudin, K. Zhang, and V. B. Eltsov, Nature Comm. **10**, 237 (2019).

25. O. T. Ikkala, G. E. Volovik, P. J. Hakonen, Yu. M. Bunkov, S. T. Islander, and G. A. Kharadze, JETP Lett. **35**, 416 (1982).

26. E. V. Thuneberg, Phys. Rev. Lett. **56**, 359 (1986).

27. G. E. Volovik and M. M. Salomaa, JETP Lett. **42**, 521 (1985).

28. Y. Kondo, J. S. Korhonen, M. Krusius, V. V. Dmitriev, Yu. M. Mukharskiy, E. B. Sonin, and G. E. Volovik, Phys. Rev. Lett. **67**, 81 (1991).

29. G. E. Volovik, JETP Lett. **52**, 358 (1990).

30. M. A. Silaev, E. V. Thuneberg, and M. Fogelström, Phys. Rev. Lett. **115**, 235301 (2015).

31. T. W. B. Kibble, G. Lazarides, and Q. Shafi, Phys. Rev. D **26**, 435 (1982).

32. G. E. Volovik and K. Zhang, arXiv:2002.07578.

33. E. Witten, Nucl. Phys. B **249**, 557 (1985).

34. V. V. Zavjalov, S. Autti, V. B. Eltsov, P. Heikkinen, and G. E. Volovik, Nature Comm. **7**, 10294 (2016).

35. G. E. Volovik, Pis'ma v ZhETF **109**, 509 (2019) [JETP Lett. **109**, 499 (2019)].

36. N. D. Mermin and T.-L. Ho, Phys. Rev. Lett. **36**, 594 (1976).

37. V. R. Chechetkin, JETP **44**, 766 (1976).

38. P. W. Anderson and G. Toulouse, Phys. Rev. Lett. **38**, 508 (1977).

39. Ü. Parts, E. V. Thuneberg, G. E. Volovik, J. H. Koivuniemi, V. M. H. Ruutu, M. Heinilä, J. M. Karimäki, and M. Krusius, Phys. Rev. Lett. **72**, 3839 (1994).

40. Ü. Parts, M. Krusius, J. H. Koivuniemi, V. M. H. Ruutu, E. V. Thuneberg, and G. E. Volovik, JETP Lett. **59**, 851 (1994).

41. V. B. Eltsov, R. Blaauwgeers, N. B. Kopnin, M. Krusius, J. J. Ruohio, R. Schanen, and E. V. Thuneberg, Phys. Rev. Lett. **88**, 065301 (2002).

42. G. E. Volovik and M. Krusius, Priroda **4**, 56 (1994).

43. Г. Е. Воловик, УФН **185**, 970 (2015).

44. L. D. Landau and E. M. Lifshitz, Doklady Akademii Nauk SSSR **100**, 669 (1955).

45. S. Blaha, Phys. Rev. Lett. **36**, 874 (1976).

46. G. E. Volovik and V. P. Mineev, JETP Lett. **23**, 593 (1976).

47. Y. Nambu, Nucl. Phys. B **130**, 505 (1977).

48. Yifung Ng, T. W. B. Kibble, and Tanmay Vachaspati, Phys. Rev. D **78**, 046001 (2008).

49. M. Krusius, A. P. Finne, R. Blaauwgeers, V. B. Eltsov, and G. E. Volovik, Physica B **329–333**, 91 (2003).

50. N. D. Mermin, in *Quantum Fluids and Solids*, ed. by S. B. Trickey, E. D. Adams, and J. W. Dufty, Plenum, New York (1977), pp. 3–22.

51. G. E. Volovik, JETP Lett. **28** 59 (1978).

52. M. W. Ray, E. Ruokokoski, S. Kandel, M. Möttönen, and D. S. Hall, Nature **505**, 657 (2014).

53. T. Sh. Misirpashaev and G. E. Volovik, ZhETF **101**, 1197 (1992); JETP **75**, 650 (1992).

54. G. Lazarides and Q. Shafi, arXiv:1904.06880.

55. T. T. Heikkilä and G. E. Volovik, New J. Phys. **17**, 093019 (2015).